

Supporting Information

Faust et al. 10.1073/pnas.1006980107

SI Methods

Slice Preparation. Female Balb/cJ mice were used for preparing ex vivo brain slices (1, 2). For extracellular recordings and live imaging studies, a mouse was anesthetized, either with pentobarbital or isoflurane, and killed. The brain was quickly extracted and placed, for 3 min, in ice-cold ($<2^{\circ}\text{C}$) artificial cerebral spinal fluid (ACSF) containing the following (mM): 126 NaCl, 26 NaHCO_3 , 10 glucose, 2.5 KCl, 2.4 CaCl_2 , 1.3 MgCl_2 , 1.2 NaH_2PO_4 , and 1 kynurenic acid, constantly gassed with 95% O_2 , 5% CO_2 ("carbogen"). The brain hemispheres were separated and dissected onto a block that was then glued to a stage for sectioning on a vibratome (Leica VT1200). Transverse hippocampal slices (350- to 400- μm thick) were cut while bathed in ice-cold ($<2^{\circ}\text{C}$) ACSF. For whole-cell recordings, slice dissection (350- μm thick) was performed in ice-cold ACSF containing the following (mM): 75 sucrose, 87 NaCl, 26 NaHCO_3 , 10 glucose, 2.5 KCl, 0.5 CaCl_2 , 7 MgCl_2 , 1.2 NaH_2PO_4 (osmolality, 300 mOsm, pH 7.2). Slices were then incubated (35°C , 35 min), allowed to equilibrate back to 25°C for 2 h, and then transferred to a recording chamber that was perfused with ACSF heated at 30°C and gassed with carbogen. All chemicals were acquired from Sigma-Aldrich.

Electrophysiology. A stimulating Pt-Ir electrode (Frederick Haer) was placed in *stratum radiatum* to stimulate the axons of the Schaffer collateral/commissural pathway. Extracellular fEPSPs were measured with a recording pipette (2 M NaCl) in *stratum radiatum* of CA1. Responses were amplified (AM-Systems 1800) and collected with laboratory-written Axobasic software (10 kHz digitization). Before recording NMDAR-mediated fEPSPs, slices were incubated for at least 5 min in Mg^{2+} -free ACSF. For whole-cell recordings, CA1 pyramidal neurons were identified visually with an upright microscope (Olympus BX50) optimized for infrared differential-interference-contrast optics. Whole-cell patch clamp recordings were done with borosilicate glass electrodes (5- to 8-M Ω tip resistance). The internal solution contained the following (mM): 115 Cs-gluconate, 10 Hepes, 0.6 EGTA, 2 MgCl_2 , 5 KCl, 4 $\text{Na}_2\text{-ATP}$, and 0.3 GTP-Tris. Synaptic whole-cell responses were amplified (Dagan), digitized (5 kHz) via AD converter (Instrutech), and stored with Pulse software (Heka). The voltage-clamp technique was used for studying NMDAR-mediated EPSCs.

NMDAR Mixture. NMDAR-mediated responses were studied in pharmacological isolation by adding the following agents to the ACSF: CNQX (20 μM , AMPAR blocker), LY367385 (100 μM , blocker of metabotropic glutamate receptor 1), MPEP (10 μM , blocker of metabotropic glutamate receptor 5), picrotoxin (100 μM , blocker of synaptic GABA_A receptors) and gabazine (10 μM , blocker of extrasynaptic GABA_A receptors), saclofen (200 μM , blocker of GABA_B receptors), methyllycaconitine (10 nM, blocker of $\alpha 7$ nicotinic receptors), and strychnine (1 μM , blocker of glycine receptors). For field recordings, slices were incubated for at least 5 min in Mg^{2+} -free ACSF, a maneuver intended to remove the Mg^{2+} block from the NMDARs so they could be activated with weak stimulation.

AMPA Mixture. AMPAR-mediated responses were isolated with the following mixture of blocking agents: AP5 (50 μM , NMDAR blocker), LY367385 (100 μM), MPEP (10 μM), picrotoxin (100 μM), gabazine (10 μM), saclofen (200 μM), methyllycaconitine (10 nM), and strychnine (1 μM).

GABAR Mixture. GABAR-mediated responses were measured with intracellular techniques and pharmacological isolation. The mixture of blocking agents consisted of CNQX (20 μM), AP5 (50 μM), LY367385 (100 μM), MPEP (10 μM), methyllycaconitine (10 nM), and strychnine (1 μM).

AAb Treatments. AAbs were synthesized in our laboratory (3). After establishing baseline synaptic responses (0.1 Hz stimulation, 10 min), AAbs were added for 10 min. The design consisted of applying AAb (R4A, G11) to a slice and control Ab (IgG2b, B1), at the same dose, to a different slice from the same animal; therefore, we generated parallel dose-response curves for both agents. Pre-treatment averaged fEPSPs ($n = 30$, 5 min before AAb) were compared with treatment responses ($n = 30$, last 5 min of AAb exposure). For voltage-clamped EPSCs, the initial responses were measured at -60 mV with the strength adjusted to obtain inward EPSCs of ~ 50 pA. Thereafter, I-V curves were measured after 8–10 min of AAb exposure.

MK-801 Synaptic Blockade and Histology. NMDAR-dependent fEPSPs were recorded in ex vivo slices using the NMDAR mixture. After obtaining a baseline response (~ 15 min), MK-801 (50 μM) was applied to the bath until the fEPSPs decayed to an amplitude near 0 mV, which took 10–15 min (Fig. S1). Once stable NMDAR blockade was accomplished, each slice was fixed in 4% paraformaldehyde and 1% glutaraldehyde in PBS for 1 h, thoroughly washed, cryoprotected in 30% sucrose, embedded in OCT Compound (Tissue-Tek), and stored at -80°C . As a control, slices were recorded in normal ACSF for 30 min before being fixed and processed. The 400- μm slices were further cut with a cryostat (Leica CM3050S) into thin sections (30–40 μm) and mounted on slides. The thin sections were postfixed in ice-cold methanol (100%) for 15 min, washed in PBS and blocked in PBS containing 10% normal goat serum. The sections were then incubated with DNase I (1 mg/mL) in PBS containing 10 mM MgCl_2 (DNase I from bovine pancreas, Type IV Sigma). Subsequently, the sections were incubated overnight at 4°C with SLE AAbs, which were visualized with infrared imaging, fluorescent immunocytochemistry, or brightfield immunocytochemistry, as described below.

Infrared Imaging. R4A (40 $\mu\text{g}/\text{mL}$) and IgG2b (40 $\mu\text{g}/\text{mL}$) were labeled with IRDye800 in PBS. Thin sections were incubated overnight at 4°C with these infrared-labeled Abs, washed in PBS, and mounted with Dako Fluorescence Mounting Medium (Dako). The sections were imaged with the Odyssey infrared imaging system (LI-COR Biosciences), which permitted measurement of infrared signals in arbitrary units.

Fluorescent Immunocytochemistry. This technique was applied to thin sections pretreated with MK-801 and also to hippocampal sections obtained from perfused mice (brain tissue was fixed, sectioned, and treated with DNase). Both types of brain sections were incubated overnight at 4°C with R4A (20 $\mu\text{g}/\text{mL}$), IgG2b (20 $\mu\text{g}/\text{mL}$), G11 (40 $\mu\text{g}/\text{mL}$), or B1 (40 $\mu\text{g}/\text{mL}$). Sections stained with R4A or IgG2b were treated with secondary FITC-conjugated antimouse Ab (Alexa Fluor 488, 1:400, Invitrogen). Sections stained with G11 or B1 were treated with FITC-conjugated secondary antihuman Ab (Alexa Fluor 488, 1:400, Invitrogen). L-glutamate was colabeled by incubation with rabbit anti-L-glutamate Ab (Sigma G6642, 1:250) and anti-rabbit secondary Ab (Rhodamine Red-X, 1:100, Jackson ImmunoResearch). Colabeling with NR2A/B was performed with rabbit anti-NR2A/B Ab (Millipore AB1548) and the antirabbit secondary Ab. In some sections, DAPI

(1:1,000, Invitrogen) was used to stain cell nuclei, as previously published (4).

Brightfield Immunocytochemistry. Brain tissue from perfused mice was fixed, sectioned, and mounted on slides. Mounted sections were treated with DNase, blocked, and stained overnight at room temperature with R4A (60 $\mu\text{g}/\text{mL}$) or IgG2b (60 $\mu\text{g}/\text{mL}$). The next day, sections were treated with biotinylated anti-mouse IgG Ab (1:200, Vector Laboratories), followed by a 1:200 solution from Vectastain Elite ABC Kit (Vector, PK-6100), and 3,3'-diaminobenzidine (DAB, 0.05%) with hydrogen peroxide (0.003%). Sections were dehydrated through graded alcohols and xylene, and cover-slipped with Permount.

TUNEL Assay. Stereotaxic injections of AAb (2 μL) were performed as previously described (5). AAb concentrations are indicated in Fig. 6. Animals were killed and perfused 24 h after injection; subsequently, brains were postfixed and cryoprotected. Hippocampal sections (40 μm thick) were microtome cut with an embedding matrix (Shandon M-1, Thermo Electron Corporation). TUNEL was performed with TACS-Tdt-Apoptosis Detection Kit (R&D #TA4625) as reported (4). TUNEL-stained tissue was visualized as described below, and TUNEL(+) cells were quantified in a volume of $1.5 \times 10^6 \mu\text{m}^3$, centered on the injection site.

Imaging of Fixed Tissue. Brain sections were imaged on an Axio-Imager microscope equipped with AxioVision 4.7.2 software (Zeiss). Transmitted light images were documented by a microscope-mounted camera (Zeiss, 12-bit, 25-MHz); in $1,388 \times 1,040$ pixel resolution and converted to eight-bit TIFF files, downloaded to Photoshop (CS2 version; Adobe), in which gray-scales were adjusted equally for all frames in a given figure. Fluorescent images were documented by a monochrome camera (MRm, Zeiss, 12-bit) and converted to false-color images (Zeiss ZVI format). The merged images taken with different fluorescent cubes were converted to eight-bit TIFF files and downloaded to Photoshop (Adobe), in which black scales were adjusted equally for all frames in a figure.

Confocal Live Imaging of mPT. Slices were transferred to an imaging chamber (RC-26GS, Warner Instruments) and secured with an anchor (Warner Instruments), with two strings removed so that the hippocampus would not be damaged. Slices were bathed with Mg^{2+} -free ACSF, heated at 30 $^\circ\text{C}$ and gassed with carbogen, for 10 min. Slices were bathed in loading solution (1 mL) containing the following (μM): 1 calcein-AM, 1,000 CoCl_2 , and 1 Hoechst 33342 (Invitrogen) in Mg^{2+} -free ACSF, for 15 min, which was followed by washout with Mg^{2+} -free ACSF (15 min); thereafter, imaging proceeded at 10-min intervals (defined as T0, T10, T20, T30, and T40). After T0 imaging, ACSF was switched to a high-

K solution containing 30 μM glycine, 35 mM KCl, 10 μM CNQX, 100 μM picrotoxin, 100 μM saclofen, and 20 μM gabazine. Concomitantly, SLE AAbs, NMDA, and other pharmacological agents were added as indicated in the text and figure legends (Figs. 4 and 5 and Fig. S5). Imaging was performed with a confocal unit (LSM510, Zeiss) fitted to an upright microscope (Axioskop 2-MOT, 40 \times W/0.8 dipping lens, Zeiss). Calcein excitation was accomplished with an argon ion laser tuned to 488 nm (Lasos LGK-7812 ML-4). DAPI excitation was accomplished with an argon ion laser tuned to 351 nm (Coherent Enterprise II). Pinhole aperture was set at 340 μm , with 100- μm z-stacks acquired at 3- μm intervals. Imaging software (Axiovision v4.7, Zeiss) was used to align the time series and quantify fluorescence.

Live Imaging Analysis. The imaged fields ($1,024 \times 1,024$ pixels) were divided into 16 subfields (224×224 pixels), each subfield corresponding to an area of $50 \times 50 \mu\text{m}^2$. Fluorescence was quantified as area (μm^2) greater than 50 arbitrary fluorescence units (range, 0–255, eight-bit). Subfields with fluorescence values less than 40 μm^2 displayed less than one cell body and were excluded from further analyses. Time series changes in fluorescence were expressed ratiometrically as a percentage of initial fluorescence (at T0).

Assays for HIF Induction and Cell Viability. A cell-based hypoxia response element (HRE)/luciferase reporter system was used to study the effect of cobalt on HIF activation and cell viability. The reporter system is based on immortalized hippocampal neuroblast cell line (HT22) transfected with a promoter-reporter construct that contains 68 bp of a known hypoxia and HIF-1-regulated gene, enolase, with a WT hypoxia response element (HRE, 5'-RCTGT-3') (6). The reporter system allows screening for a broad spectrum of compounds that include activators of HIF transcription, activators of HIF binding to HRE, and effectors of HIF protein stability (PHD inhibitors, pVHL, and proteasome inhibitors).

Cells were plated at a density of 10,000 cells per well using a WellMate multichannel dispenser from Matrix (Thermo Fisher Scientific) and grown overnight on DMEM (high glucose 1 \times , Gibco 11965; 100 mL per well). Aliquots (10-mL) containing varied concentrations of cobalt chloride (CoCl_2 , 0.06–1 mM) were added to the wells from a preliminary prepared masterplate using an epMotion 5070 station from Eppendorf. The plates were incubated for 30 min and 75 min, and then the medium was removed, cells lysed and luciferase activity measured with BrightGlo reagent from Promega in accordance with the manufacturer's protocol. Cell viability test was performed by simultaneous plating in the 96-well plates with transparent bottom and subsequent morphological assay, which involves simply observing the cells by phase-contrast microscopy.

1. Chang EH, et al. (2006) AMPA receptor downscaling at the onset of Alzheimer's disease pathology in double knockin mice. *Proc Natl Acad Sci USA* 103:3410–3415.
2. Chang EH, Rigotti A, Huerta PT (2009) Age-related influence of the HDL receptor SR-BI on synaptic plasticity and cognition. *Neurobiol Aging* 30:407–419.
3. Zhang J, et al. (2008) Identification of DNA-reactive B cells in patients with systemic lupus erythematosus. *J Immunol Methods* 338:79–84.

4. Lee JY, et al. (2009) Neurotoxic autoantibodies mediate congenital cortical impairment of offspring in maternal lupus. *Nat Med* 15:91–96.
5. DeGiorgio LA, et al. (2001) A subset of lupus anti-DNA antibodies cross-reacts with the NR2 glutamate receptor in systemic lupus erythematosus. *Nat Med* 7:1189–1193.
6. Aminova LR, et al. (2005) Prosurvival and prodeath effects of hypoxia-inducible factor-1 α stabilization in a murine hippocampal cell line. *J Biol Chem* 280:3996–4003.

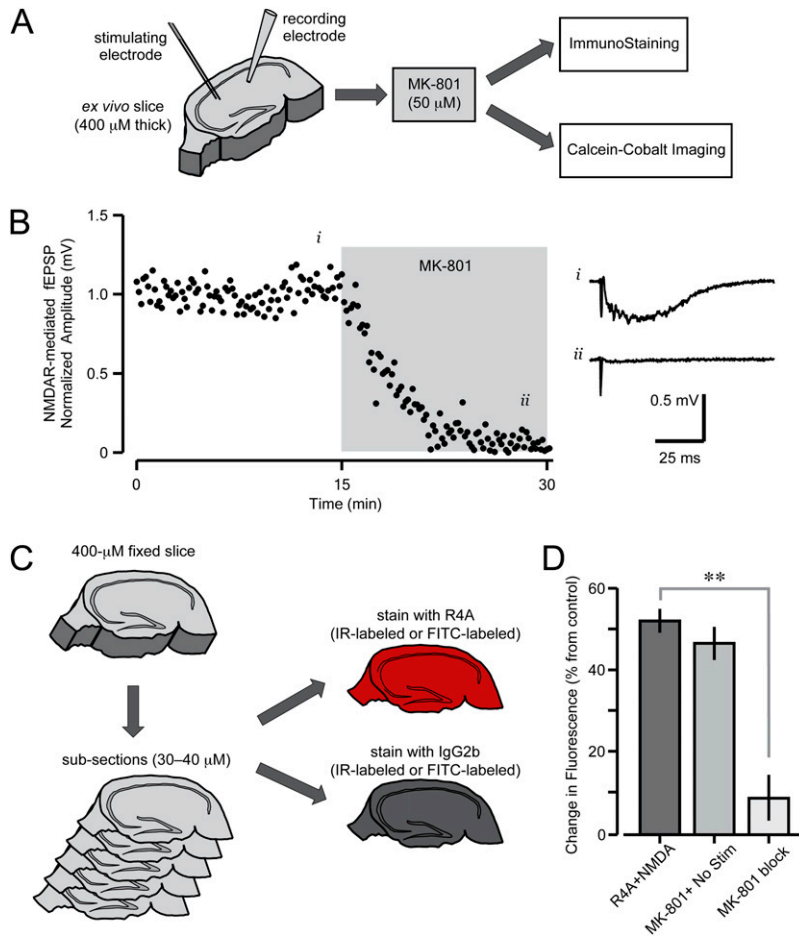


Fig. S1. Blockade of synaptic NMDARs by MK-801. (A) Block diagram of setup for synaptic recordings, with subsequent MK-801 block, staining, and imaging. (B) Application of MK-801 (50 μM) while the synapses are activated (0.1 Hz stimulation), marked by gray box, leads to complete blockade of NMDAR-mediated fEPSPs in CA1. (Right) Traces correspond to NMDAR-mediated fEPSPs before blockade (*i*, Upper) and postblockade (*ii*, Lower). (C) Diagram of subsectioning of fixed slices, and subsequent staining with infrared-labeled Abs or FITC-labeled Abs. (D) R4A (200 $\mu\text{g}/\text{mL}$) treatment following synaptic blockade by MK-801 displays attenuation of mPT compared with unblocked group (R4A + NMDA vs. MK-801 block, $T = 8.5$, $**P < 0.001$, t test). Notice the lack of protection in the group with synaptic blockade without concurrent synaptic stimulation (MK-801 + No Stim).

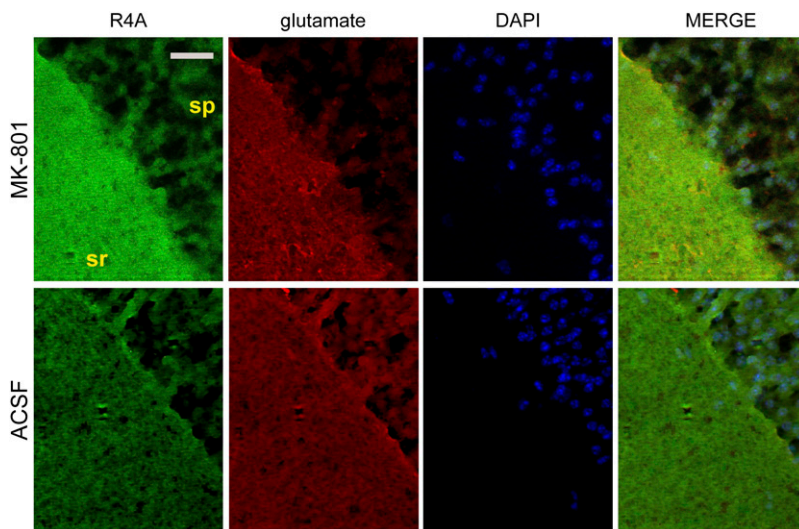


Fig. S2. Robust R4A binding in hippocampal sections pretreated with MK-801. (Upper) Section of CA1 region after functional NMDAR blockade by MK-801 (described in Fig. S1) displays colocalized R4A, DAPI and glutamate signals, as evidenced in Merge panel. (Lower) CA1 section treated with ACSF only (not MK-801 blockade) also shows colocalized signals. Notice the stronger R4A labeling in the MK-801 pretreated section. (Scale bar: 20 μm .) *sp*, stratum pyramidale; *sr*, stratum radiatum.

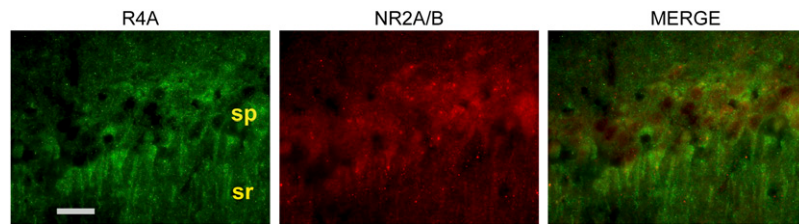


Fig. S3. Colocalization of R4A and NR2A/B labeling within CA1 pyramidal cells. (Scale bar: 20 μm .) sp, stratum pyramidale; sr, stratum radiatum.

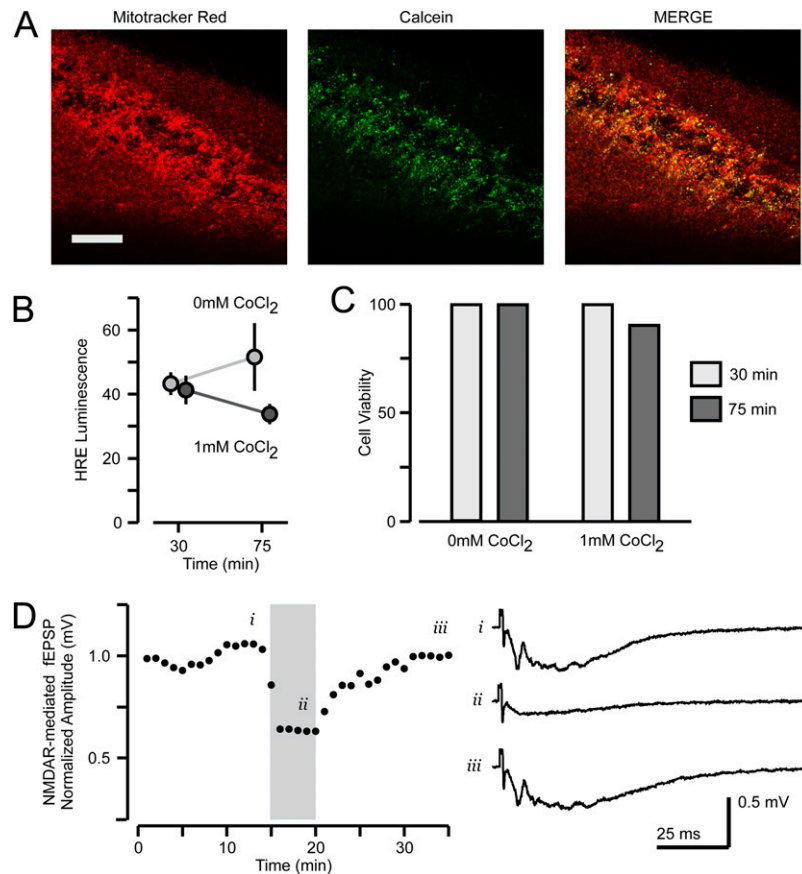


Fig. S4. Validation of calcein/cobalt method for monitoring mPT. (A) Colocalization of calcein with mitotracker red in cell bodies of CA1 pyramidal cells following loading with calcein AM (1 μM), CoCl₂ (1 mM), and mitotracker red (0.2 μM). (Scale bar: 50 μm .) (B) HIF induction (mean \pm SD) following 15 min CoCl₂ (1 mM) incubation. CoCl₂ was washed out following incubation. Time points represent 30 min and 75 min post-CoCl₂ incubation. The y-axis scale corresponds to arbitrary fluorescence units. (C) Cell viability of HT22 cultures following exposure to 1 mM CoCl₂, following the same time points as in B. (D) Application of CoCl₂ (1 mM, during period indicated by gray bar) temporarily depresses NMDAR-mediated fEPSPs. Traces correspond to NMDAR-mediated fEPSPs before CoCl₂ application (*i*, Top), during CoCl₂ bath (*ii*, Middle), and following washout of CoCl₂ (*iii*, Bottom).

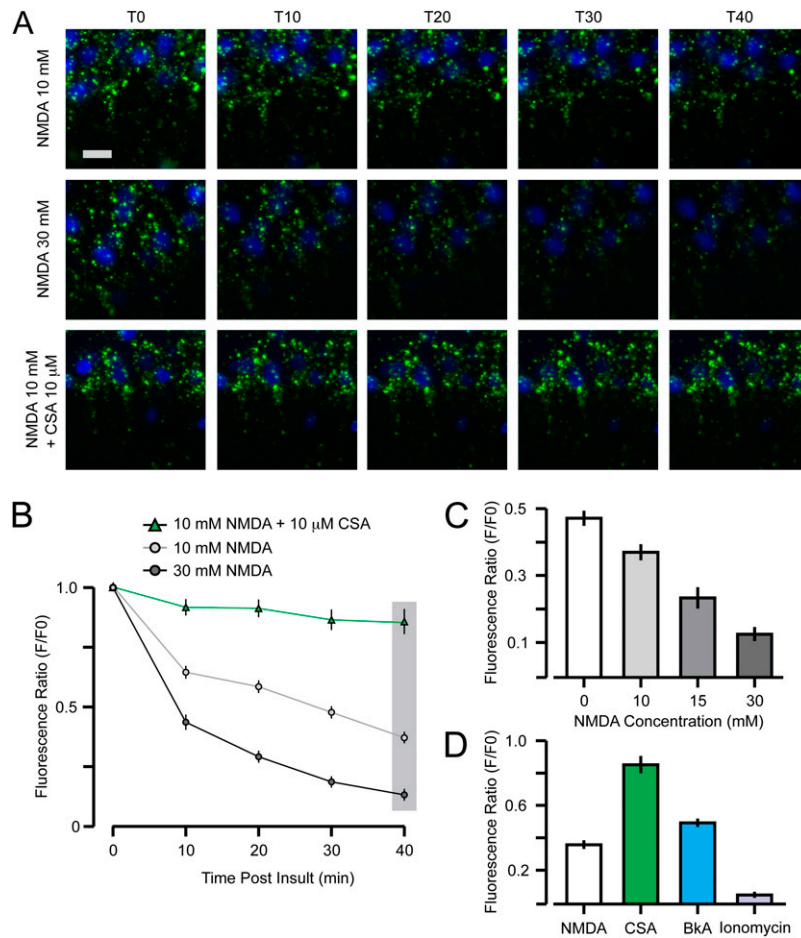


Fig. S5. NMDA-induced mPT in *stratum pyramidale* of CA1. (A) Sample fluorescent micrographs during treatment with NMDA (10 mM, 30 mM), and with CSA (10 μ M); time (T) is given in minutes. (Scale bar: 10 μ m.) (B) Quantitative fluorescence decay profiles (mean \pm SD) of treatments shown above. (C) Graph (mean \pm SD) shows mPT induced by increasing NMDA concentrations plotted at 40 min after insult (T40), marked by gray area in B. (D) Graph (mean \pm SD) shows blockade of NMDA-induced mPT (10 mM NMDA) with mPT inhibitors cyclosporine A (CSA, 10 μ M), and bongkreik acid (BkA, 70 μ M) at T40. Ionomycin (0.5 μ M) was also observed to induce rapid mPT (T10 value, instead of T40, is shown).